Environment and Natural Resources Research; Vol. 4, No. 4; 2014
ISSN 1927-0488 E-ISSN 1927-0496
Published by Canadian Center of Science and Education

Landscape Mapping to Quantify Degree-of-Freedom, Degree-of-Sprawl, and Degree-of-Goodness of Urban Growth in Hawassa, Ethiopia

Nigatu Wondrade[1, 2], Øystein B. Dick[1] & Håvard Tveite[1]

[1] Norwegian University of Life Sciences (NMBU), Department of Mathematical Sciences and Technology, P. O. Box 5003, N-1432, Ås, Norway

[2] Department of Biosystems & Environmental Engineering, Institute of Technology, Hawassa University, P. O. Box 5, Hawassa, Ethiopia

Correspondence: Nigatu Wondrade, Norwegian University of Life Sciences, Department of Mathematical Sciences and Technology, P. O. Box 5003, N-1432, Ås, Norway. Tel: 47-6496-6394, 251-934-751-455. E-mail: nigatwond@yahoo.com, nigatu.tedo@nmbu.no

Received: September 3, 2014 Accepted: October 17, 2014 Online Published: October 27, 2014

doi:10.5539/enrr.v4n4p223 URL: http://dx.doi.org/10.5539/enrr.v4n4p223

Abstract

In the rapidly urbanizing African continent, monitoring, mapping and modeling of urban growth is an indispensable task to understand the magnitude and rate of the ongoing changes. Remote sensing data have been found useful in mapping urban areas and as a source of data for modeling and analysis of spatio-temporal trajectories of cities. In this study, remote sensing data from different sensors extending over a period of 24 years (1987-2011) were used to classify and extract areas of the established land use land cover classes in Hawassa City, Ethiopia. Among those classes, built-up areas were used to quantify urban growth and sprawl. The result of the mapping indicated that the built-up area had increased by 234.5% between 1987 and 2011. The area under investigation was sub-divided into eight equal zones within a circle to apply analytical models. To analyze the pattern, process and overall growth status of Hawassa City, Pearson's Chi-square statistics, Shannon's entropy, and degree-of-goodness models were employed. The result revealed that the degree-of-freedom was high indicating the disparity between observed and expected urban growth. The entropy values both in temporal intervals and zones were found higher than half-way mark of $log_e(n)\ or\ log_e(m)$ respectively showing the tendency of sprawl. Except the South Zone, the city had not experienced "goodness" during the entire study period. This study has provided new evidence about the urban growth in the study area that could be used by city managers.

Keywords: Hawassa, GIS, remote sensing, urban growth, urban sprawl

1. Introduction and Background

Urban growth is an important global environmental issue that affects both developed and developing countries (Grey, Luckman, & Holland, 2003). Africa is one of the continents where the most explosive urban growth (30-35%) is underway, at a roughly 4% per annum. Consequently, Africa is expected to be about 54% urban by 2025 (World Resources [WR], 1996).

Between 1990 and 2025, the number of people living in urban areas is also expected to be more than five billion and from all of this growth, a staggering 90%, will occur in the developing countries (ibid).

Though there are about eight cities in Ethiopia that are all highly populated, Hawassa is special in that it is the youngest and a multi-ethnic city in South Ethiopia. The high rate of population growth and urban expansion, particularly in the last two decades, attracted our attention.

The population of Hawassa increased from 41 138 in 1987 to 313 564 in 2011 (Central Statistical Agency [CSA], 1988 & 2011). This puts Hawassa in the medium-sized city category with a population between 100 000 and 500 000 (Zanganeh et al., 2011). Rural-to-urban migration and natural growth are the causes for the population growth in Hawassa (ALLREFER, 1991; Aynalem, 2011), though the late merging of the nearby villages as it developed also contributed to some extent.

According to the Central Statistical Agency of Ethiopia (2011), urban area refers to all capitals of regions, zones and *"weredas"*/districts, and localities with urban *"kebeles"* whose inhabitants are primarily engaged in non-agricultural activities. Hawassa is the capital of Southern Nations Nationalities and Peoples Regional State (SNNPRS) and one of the fastest growing cities in Ethiopia (Hurni, Bantider, Herweg, Portner, & Veit, 2007; Wondrade, Dick, & Tveite, 2014). The definition of urban area given by CSA associates urban growth mainly with non-agricultural activities and this definition lacks spatial and population dimensions. Bhatta, Saraswati, & Bandyopadhyay (2010a) defined urban growth as a spatial and demographic process which occurs when the population distribution changes from being largely hamlet and village based to being predominantly town and city dwelling. Changes in urban areas are dynamic and require regular monitoring to understand the overall changes for proper planning and allocation of resources. Effective planning policy and appropriate resource management can only be accomplished through informed decisions, but even basic information on urban extent and change is often outdated, inaccurate, or simply does not exist (Grey et al., 2003) and this is common in developing countries.

We have witnessed that the recent rapid urban growth in the area has created pollution of water resources (Abebe & Geheb, 2003), reduction of agricultural land, shortage of shelter, and opening a lee way for invasion of public land by squatters. In the last 10 years, more attention has been paid to urban land use land cover (LULC) changes due to the fact that urban ecosystems are strongly affected by anthropogenic activities and have close relations with the life of almost half of the world's population (Xiao et al., 2006). To sustain such rapid changes in urban growth, development planning is indispensable. This, in turn, demands proper monitoring of the changing environment and this research was initiated to address such demands. The most effective way to monitor LULC changes and analyze the dynamics of urban spatial growth is through the use of remote sensing data. That is why we directed our efforts, in this study, to use of remote sensing data in combination with Global Positioning System (GPS) data to classify and extract LULC data. However, change detection from classified images alone was not enough to quantify the degree of sprawl (dispersion) or compactness of the urban growth. Thus, the remote sensing community has developed analytical models, using Chi-square statistics (Almeida et al., 2005), Shannon's entropy (Yeh & Li, 2001), and degree-of-goodness (Paul & Dasgupta, 2013) to quantify the spatial patterns and processes of urban growth over time.

Literature review found that several studies were conducted to quantify urban growth and sprawl covering pattern (Sudhira, Ramachandra, & Jagadish, 2004; Ji, Ma, Twibell, & Underhill, 2006; Jat, Garg, & Khare, 2008; Sarvestani, Ibrahim, & Kanaroglou, 2011), process (Galster et al., 2001; Bhatta et al., 2010b; Bhatta, 2012), and an overall analysis (Bhatta et al., 2010a) that combines both pattern and process. Bhatta (2012) specifically indicated that urban change detection focus has shifted from detection to quantification of change, measurement of pattern, and analysis of pattern and process of urban growth and sprawl. In this study, we also used pattern, process, and an overall analysis to quantify urban growth status. Urban growth as a pattern refers to the spatial configuration of built-up areas in each temporal instant while the process reveals the changes in spatial structure of cities over time. Thus, urban growth analysis that takes into account both pattern and process will help us to understand the changes in built-up area in space and time, including the presence or absence of sprawl. Sprawl, as Galster et al. (2001) described, is a metaphor rich in ambiguity that bears one name for many conditions. This has emanated from the lack of agreement among scholars on its definition (Johnson, 2001). For the current study, we consider urban sprawl as uncontrolled, scattered sub-urban development that increases traffic problems, depletes local resources, and destroys open space (Ji et al., 2006).

In Africa, more than 10 years ago, spatial analysis capabilities were limited (Karanja, Heipke, & Konecny, 2002). Literature review also has not found any research output related to urban growth analysis in the study area and probably this could be the first documentation of the changes in urban dynamics in Hawassa. Generally, the advent of remote sensing data and associated software packages has created an opportunity to quantify LULC data and to model urban growth/sprawl using selected spatial models. The main objective of this study was, therefore, twofold. First, we aimed to detect and quantify LULC classes and output cover maps. Our second aim was to examine the spatio-temporal growth status of Hawassa City for the time interval between 1987 and 2011. The specific objectives include: (1) to classify and extract the proportion and magnitude of built-up areas, (2) to identify and utilize spatial models for quantifying urban growth and sprawl i.e., (i) to quantify the rate of urban growth, (ii) to test the relationship between observed and expected growth (degree-of-freedom), (iii) to analyze whether the growth was sprawling or not using Shannon's entropy, and (iv) to estimate the overall degree-of-goodness and produce a detailed report of urban growth status for further use. We hope that this study will give an insight in the past and present urban growth situation in Hawassa and even be used as a basis for future growth analysis by all people who have a stake in the city.

2. Materials and Methods

2.1 Study Area Description

Hawassa, formerly known as Awassa, is the capital city of SNNPRS, Ethiopia. It is located 275 km south of Addis Ababa along the main highway leading to Nairobi, Kenya via Moyale. This study area (Figure 1) lies between $6^o55' - 7^o06'N$ Latitude and $38^o25' - 38^o33'E$ Longitude and the altitude ranges from 1656 to 2137 m above sea level. The Hawassa City Administration covers an area of 16 062 hectares (ha) and is sub-divided into eight Sub-Cities and 32 "Kebeles". The research area has a favorable climate with an annual mean minimum and maximum temperature of 13.0°C and 29.2°C respectively and 975.9 mm mean yearly precipitation estimated for ten years using meteorological data.

Hawassa obtained its beauty and name from the Lake Hawassa situated in the Main Ethiopian Rift Valley. However, the availability of water and grazing land had been a major source of conflict among the pastoral community inhabited in this area. The Hawassa city was founded relatively recently (1960) succeeding Yirgalem to become a capital of the former Sidama Province (Zeleke & Serkalem, 2006; Assefa, Alemu, & Abinet, 2011). Then, in late 1970s, it was decided to establish Hawassa as the seat of former four administrative regions in the south, namely Arsi, Bale, Gamo Gofa, and Sidama. However, significant growths including built-up areas have been observed since 1994, when Hawassa became the capital of SNNPRS and the Sidama Zone. The population of Hawassa in 1960 was estimated between 2 500 and 3 000 (Zeleke & Serkalem, 2006). The population of Hawassa projected for 2012 based on the 2007 Census of Ethiopia has grown to 315 459 (Bureau of Finance & Economic Development [BOFED], 2011). The city is now housing a number of industries and institutions attracting people not only within the region, but also all over the country. Accordingly, the demand for housing and other amenities is higher than ever.

Comparing the yearly built-up growth rate (9.8%) estimated from the remote sensing data and yearly population growth rate (27.6%) for 1987-2011, the urban growth would be expected to much greater to cope with the housing demands of the growing population.

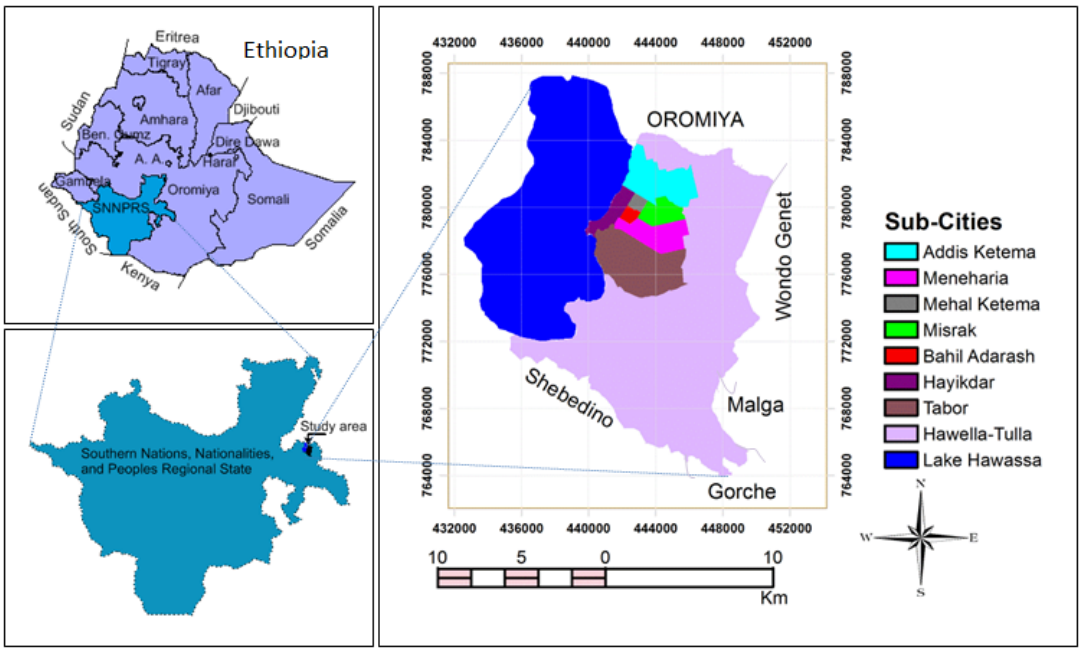

Figure 1. Map showing the study area with sub-cities and neighboring districts

2.2 Image Data Sets and Ancillary Data

High resolution image data such as IKONOS and QuickBird are the most suitable for urban landscape mapping. But, due to budget constraints and at some points their unavailability, this study used SPOT and Landsat imagery to extract built-up areas.

Landsat image data was downloaded from the Website, Global Visualization Viewer at http://glovis.usgs.gov, while the SPOT image data were procured from *e-geos*, an Italian Space Agency and Telespazio Company. The main characteristics of the imagery are described in Table 1. The dates of imagery have been selected in order to estimate LULC changes of 12 years temporal intervals. The three image data sets used were obtained geometrically corrected and projected to the standard Universal Transverse Mercator (UTM) coordinate system (WGS 84 datum, Zone 37N).

Some additional ancillary data were used to assist image interpretation and optimum information extraction from the remotely sensed data.

Table 1. The main characteristics of the utilized satellite images

Acquisition Date	Satellite and Sensor	Spatial resolution (m)	Spectral bands considered
20 January 1987	SPOT1-HRV2	20x20	1, 2, 3
25 January 1999	Landsat5-TM	30x30[a]	1, 2, 3, 4, 5, 7
22 March 2011	SPOT4-HRVIR2	20x20	1, 2, 3, 4

[a] Processed spatial resolution.

These include: a topographical map with scale 1:50 000 obtained from the Ethiopian Mapping Agency, QuickBird image data supplied by e-geos Company, and ground-truth data collected in the field using a hand held GPS device. The topographical map from 1988 was used to select training pixels for classification and reference points for accuracy assessment for the SPOT-1987 data. There were no topographical maps and aerial photographs within the same year as that of the image from 1999 to be used as an ancillary data. This is a common problem in developing countries. Therefore, the classification and thematic map accuracy assessment for the 1999 image data was performed using high resolution QuickBird image data from 2003. Classification and accuracy assessment for the image in 2011 was entirely performed using training pixels and reference points surveyed during the field work.

2.3 Classification Scheme

Once all the images were available, target LULC categories were established to perform classification. To create a closer correspondence between the thematic maps, seven categories were considered: built-up, water, agricultural land, vegetation, grassland, swamp, and bare land. Built-up area covers all developed areas including residential, commercial, industrial, and transportation infrastructures. Water body is open lake, river, and oxidation ponds. Agricultural land encompasses land with crop, ploughed, and fallow land. Vegetation class is a land covered by forest patches, woodland, shrubs, scattered trees mixed with grass, and perennial crops. Grassland involves area dominated by herbaceous vegetation. Swamp corresponds to areas where the water table is near or above the land surface. The existence of herbaceous vegetation is also evident in swampy area. Bare land is an area with no or scant vegetation, quarries, beachside, and exposed rocks.

2.4 Image Pre-Processing

The images considered for analysis were obtained geometrically and radiometrically corrected by the providers. However, owing to the different standards and references used by the image data set suppliers, images were co-registered to overcome the problem of mismatching when overlaying. It is important to mention that the thermal band in Landsat was excluded when stacking all the reflective bands into a single multi-band image. This is because of its coarse resolution and uncertainties that may crop up when resampling to higher resolution to match the other bands. The QuickBird image was first co-registered with the topographical map and, then all the three images were co-registered with respect to QuickBird. The transformation process was performed using ground control points (GCP) collected by GPS and it was achieved with a Total Root Mean Square Error (RMSE) of $\approx$1.04 which is slightly above the conventional requirement of less than one pixel (Mas, 1999; Rozenstein & Karnieli, 2011). To retain the original pixel values and avoid the loss in spatial detail, resampling of Landsat image data to match with spatial resolution of SPOT image was performed using nearest-neighbor resampling method. This will permit images from different sensors to match when overlaying and allow the comparison of LULC types. A vector file was then imported into ERDAS Imagine to subset each image to include only the study area for classification.

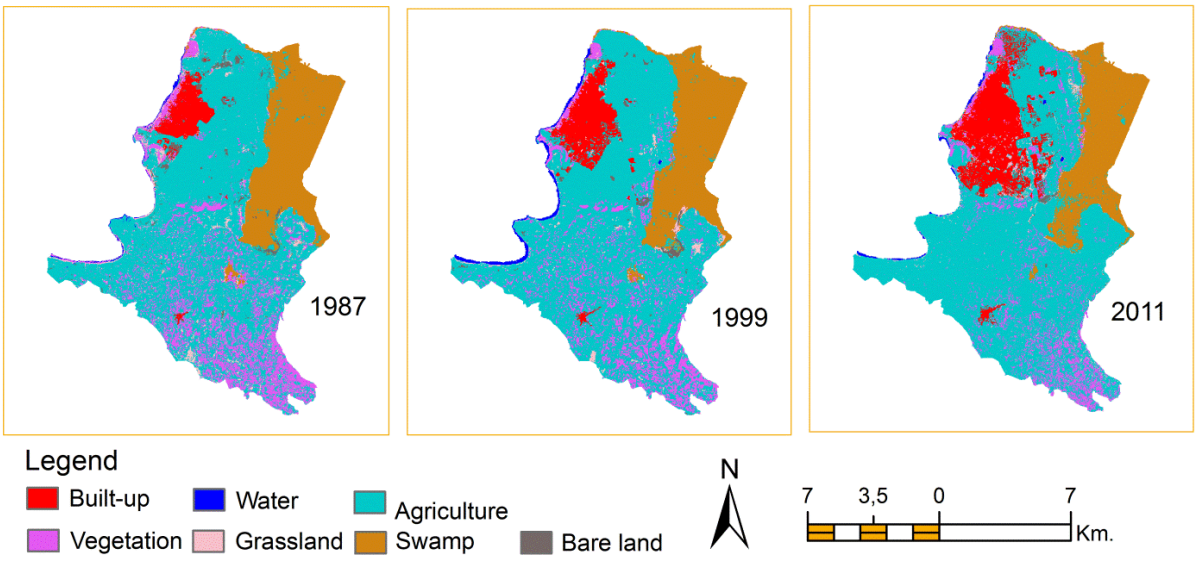

Figure 2. Thematic maps of the study area

2.5 Image Classification

Classification of a heterogeneous urban surface with a complex combination of features is a challenging task, particularly when using coarse spatial resolution images. This was also our experience, and it was not possible to separate all the LULC classes. To overcome these limitations, the image data sets were sub-divided into several landscape units to discern the LULC classes. Accordingly, based on visual inspection and ancillary data, images from 1987, 1999, and 2011 were sub-divided into 24, 45, and 29 segments respectively to enhance classification.

Each segment was first classified using unsupervised *Iterative Self-Organizing Data Analysis Technique* (*ISODATA*) (ERDAS, 2010), allowing a large number of classes (30) to later be aggregated into the pre-defined LULC classes. Even within these relatively small segments, some misclassifications were observed. The major misclassification was between built-up area and agricultural land. This problem was attributable to the fact that building roofs, some pavements, and agricultural lands were captured by sensors with similar spectral signatures. It was also recognized that some quarries and gravel pits, the effects of anthropogenic activities, were confused with built-up areas and agricultural land. Perennial crop fields were also other sources of misclassification with vegetation cover and crop land.

In order to avoid an over/under estimation of built-up area which is the main focus of this study, the unsupervised classification was followed by the supervised maximum likelihood classification method. This permits further definition of LULC classes generated by unsupervised method (ERDAS, 2010) and yields optimum results.

An average of 105 training pixels representing the pre-defined LULC categories was selected in each image to delineate training polygons to perform supervised classification. The training pixels for SPOT-1987 and Landsat-1999 were selected from ancillary data while training pixels for the image in 2011 were collected in the field using GPS device. The training pixels were converted into vector files in a GIS environment and overlaid with the satellite image to delineate training polygons for each category. Misclassifications in the set of classes generated during unsupervised classification were refined by supervised method using the polygons delimited around the created training pixels.

Classification of all segments was performed by a hybrid method using ERDAS Imagine 2011 and the classified segments were recoded and mosaicked to form the whole. To smooth the classified images from mixed and salt-and-pepper effect which are common problems when using medium spatial resolution image data (Sarvestani et al., 2011), a majority filter with an operating window size of 3x3 was applied (Mather, 1987; Lillesand & Keifer, 2000). The classified images (Figure 2) were then exported to ArcGIS 10.1 for map presentation.

2.6 Accuracy Assessment

An accuracy assessment of the thematic maps was conducted using the reference points collected independent of the training data. Owing to significant variation in class sizes and importance, a stratified random sampling scheme was pursued to collect 256, 270, and 280 reference points to assess the accuracy of the maps from 1987, 1999, and

2011 respectively. Reference points to assess the maps from 1987 and 1999 were collected from ancillary data while these points for the map in 2011 were collected during field work using GPS. The number of reference pixels is an important factor in determining the accuracy of the classification and it has been described that a minimum of 30 samples per map class are required to adequately populate an error matrix (Congalton, 2001). The accuracy assessment was run in ERDAS Imagine 2011 to create confusion matrices for each map and accuracy measures are presented in Table 2. The overall accuracies were found above 85%, a cutoff adopted as acceptable results (Congalton & Green, 2009). The accuracies for built-up area were all above 86%. The magnitude and proportion of each land cover class with the attained accuracy is given in Table 3.

Table 2. Accuracy assessment results of the classified image data

LULC Class	1987		1999		2011	
	PA (%)	UA (%)	PA (%)	UA (%)	PA (%)	UA (%)
Built-up	88.6	88.6	92.5	90.2	86.7	86.7
Water	93.3	93.3	95.0	95.0	95.2	95.2
Agriculture	84.2	86.5	87.5	85.4	83.5	84.5
Vegetation	83.7	80.0	86.7	86.7	85.7	83.7
Grassland	79.0	75.0	80.0	75.0	86.7	76.5
Swamp	87.5	91.3	90.0	95.7	90.4	92.2
Bare land	80.0	76.2	80.0	84.2	80.0	84.2
Overall accuracy		*85.2*		*88.2*		*86.4*
Overall kappa statistics		*81.8*		*85.4*		*83.3*

Note: PA and UA stand for producer's accuracy and user's accuracy respectively.

To apply the selected models for urban growth analysis, the center point of Hawassa City was first identified. There were several locations such as, "Addis Ababa Sefer", "Harar Sefer", "Korem Sefer", "Mehal Ketema" etc., where people began to settle. But the City Center, formerly known as "Piazza" is the place where peak movement of people and business was observed (Zeleke and Serkalem, 2006). The identified center point lies between the city center building and "Sidama Bahil Adarash" or Hall. Taking this point as a center, a circle with a radius of 16 684 m was drawn, inscribing the city with built-up areas. The circle with an area of 874.46 km^2 (87 445.78 ha) was then divided into eight equal pie sections, here after referred to as zones (109.31 km^2 or 10 930.72 ha each) as North (N), North East (NE), East (E), South East (SE), South (S), South West (SW), West (W), and North West (NW) as depicted in Figure 3. A vector file with the eight subdivisions was imported into ERDAS imagine to subset the classified images for the three study points in time. The built-up areas in different directions at equal distance from the city center were then extracted in order to analyze the growth status of the city.

Table 3. Magnitude and proportion of LULC types

LULC Class	1987		1999		2011	
	(ha)	(%)	(ha)	(%)	(ha)	(%)
Built-up	600.9	3.7	1014.9	6.3	2009.8	12.5
Water	62.6	0.4	206.2	1.3	76.4	0.5
Agriculture	9632.1	60.0	9929.7	61.8	10017.4	62.3
Vegetation	2239.7	13.9	1718.0	10.7	1163.8	7.3
Grassland	340.4	2.1	195.6	1.2	167.5	1.0
Swamp	3017.2	18.8	2834.4	17.7	2600.3	16.2
Bare land	170.9	1.1	154.4	1.0	34.5	0.2
Total[b]	*16063.8*	*100.0*	*16053.2*	*100.00*	*16069.7*	*100.00*

[b] The variation in total area is due to the difference in spatial resolution and segmentation of the images.

2.7 Zoning Built-Up Spread Pattern for Analysis

Urban growth is a dynamic phenomenon which changes over time and Hawassa city has now eight sub-cities. The jurisdictional boundary of the city is much larger than the built-up area and most of the developed areas are concentrated in the seven sub-cities which cover only 24% of the city. The expansion of the city is more skewed to North-East, East, South-East, and South leaving all corners with no built-up coverage. Considering a sub-division based on administrative boundaries was not found feasible as the largest sub-city with 76% coverage was the least developed area. The extracted built-up areas of the respective zones from each temporal instant are given in Table 4 for analyzing degree-of-freedom, sprawl, and degree-of-goodness in urban growth.

3. Results and Discussion

3.1 Built-Up Area Extent and Urban Growth

Understanding a dynamic phenomenon, such as urban growth/sprawl, requires LULC change analysis, urban sprawl pattern identification and computation of landscape metrics (Jat et al., 2008).

The accuracy assessment results (Table 2) for all the available images indicated that built-up areas were classified with an accuracy of above 86%. Envisaging the growing demand of land for built-up area, the city boundary was redefined to exceed the built-up area where the total agricultural land is still the most dominant LULC category. Due to the heterogeneity of urban land cover and the coarse spatial resolution of the image data utilized, spectral confusion was observed during classification. Particularly, this was noticeable in grassland cover which was difficult to discern from vegetation and agricultural land.

Some unexpected misclassifications were also seen between built-up areas and agricultural land, attributable to very similar spectral signatures. It is also worth mentioning that certain locations with built-up cover in 1987 were seen as vegetation or agricultural land in 1999 and later. This was because of inundation of the surrounding area by Lake Hawassa that entailed the demolition of houses and evacuation of the area. Most conversions to built-up areas come from agricultural land- 33% and 47% during the 1987-1999 and 1999-2011 temporal intervals respectively. On the other hand the increase in agricultural land, though it is small, indicated that there were still conversions to agricultural land within the boundary of the city administration.

The generated maps and field observations showed that the expansion of built-up area was concentrated in the N, NE, E, SE, and S parts due to the presence of geographical barriers in the other zones. The study area is limited to the North by another state (Oromiya), to the West by Lake Hawassa, to the East by Swamp and to the South West by hills which are not suitable for urban development. Thus, the areas left for urban expansion were the North-South line along the highway and the entire Eastern and Southern part. Infill of the open spaces has also taken place in areas initially reserved for green parks, impairing the environmental and aesthetical quality of the city.

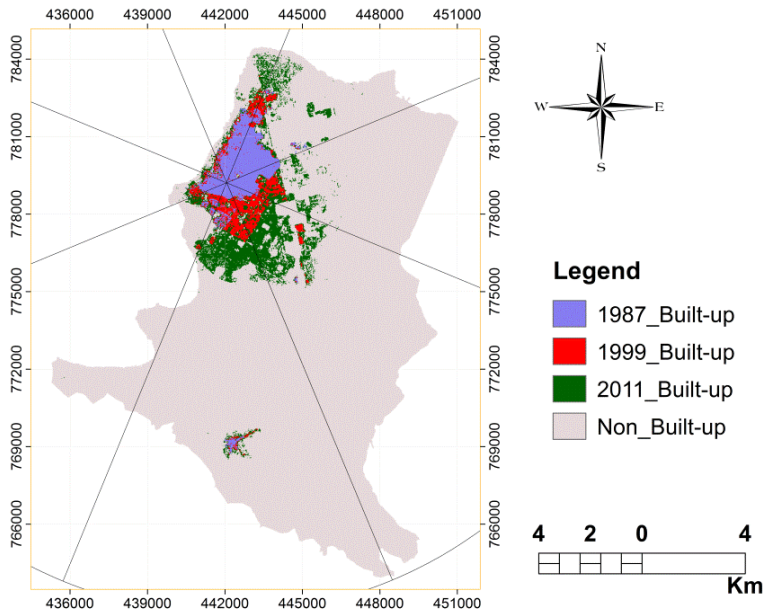

Figure 3. Overlay of classified images showing the built-up and non-built-up areas

The built-up areas for every zone in each year are presented in Table 4 along with a radar chart (Figure 4). It is worth to note that for the radar chart, 16 equal zones were used instead of eight for better visualization of the urban expansion. The chart displays an overlay of built-up areas in each temporal interval and the trends of change over time. It is also evident from the chart that the expansion of built-up areas to the left of N-S line was more or less static due to the natural barriers (lake and hills). As shown in Figure 3, the pattern of observed urban growth varies from one urban place to another and high density growth pattern dominates the area around the center point. The observed pattern explains the spatial distribution of built-up areas in each temporal instant and the process represents the change in spatial distribution of the developed areas.

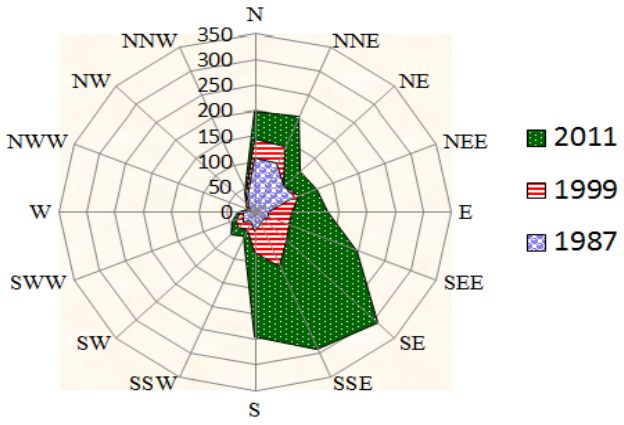

Figure 4. Radar chart showing built-up area expansion (in ha) for the three years

The observed growth in built-up area (Table 5) was computed for the two temporal intervals, 1987-1999 and 1999-2011. We can see the spatial pattern of built-up areas from the classified images, but to quantify and explain the variations in the patterns of urban growth statistically, we need to apply selected quantitative models.

Table 4. Built-up areas in each zone and each temporal instant (ha)

	N	NE	E	SE	S	SW	W	NW	The City[c]
1987	137.84	176.56	95.88	43.32	60.92	45.80	40.00	20.00	620.32
1999	186.36	210.20	146.12	142.44	189.36	77.36	59.64	30.52	1042.00
2011	247.96	317.12	246.60	495.40	527.72	109.12	71.08	33.40	2048.40

[c] *Subdividing the area into eight pie sections entailed minor changes in built-up areas*

Table 5. Observed growth in built-up areas (ha)

	N	NE	E	SE	S	SW	W	NW	Row total
1987-1999	48.52	33.64	50.24	99.12	128.44	31.56	19.64	10.52	421.68
1999-2011	61.60	106.92	100.48	352.96	338.36	31.76	11.44	2.88	1006.40
Column total	110.12	140.56	150.72	452.08	466.80	63.32	31.08	13.40	1428.08

The percentage of an area covered by impervious surfaces is a straight forward measure of urban growth (Barnes, Morgan, Roberge, & Lowe, 2002). The percentage of built-up area, as a measure of urban growth rate, was calculated for 12 years each (Table 6). The result reveals that the general trend of percentage growth rate was rising though there were decreasing rates in some zones. The highest and the lowest growth rates observed were 247.80% and 9.44% respectively (Table 6). Though the overall growth rate was increasing, that was not enough evidence to say the city was developing in the expected pattern or not which calls for further investigation.

Table 6. Percentage built-up growth rate

	N	NE	E	SE	S	SW	W	NW	The city
1987-1999	35.20	19.05	52.40	228.81	210.83	68.91	49.10	52.60	67.98
1999-2011	33.05	50.87	68.77	247.80	178.69	41.05	19.18	9.44	96.58

3.2 Pearson's Chi-Square Statistics and Urban Growth

Different from industrialized nations, some cities in developing countries lack proper planning policies and projected expectations (Paul & Dasgupta, 2013). In the absence of such policies, it was useful to apply Pearson's chi-square statistics to estimate the theoretical expected urban growth. Pearson's Chi-square statistics (degree-of-freedom) takes into account the checking of freedom amongst pairs of variables selected to explain the same category of land cover change (Almeida et al., 2005; Bhatta et al., 2010a; Bhatta, 2012). To perform the chi-square test, predefined expected values should be available but that is not the case in Hawassa city. Therefore, to compare the observed growth and expected growth, the theoretical expected urban growth was computed statistically using Equation (1). Let the Table 5 be matrix M with elements M_{ij}, where $i = 1, 2, \ldots, n$ (specific temporal intervals, rows of the table) and $j = 1, 2, \ldots, m$ (specific zones, columns of the table). The expected built-up growth for each variable was calculated by the products of marginal totals, divided by the grand total (ibid). Thus, the expected growth (M_{ij}^E) for the i^{th} row and j^{th} column is:

$$M_{ij}^E = \frac{M_i^S \, x \, M_j^S}{M_g} \quad (1)$$

$$where\ M_i^S = row\ total$$

$$M_j^S = column\ total, and$$

$$M_g = grand\ total = \sum_{i=1}^{n}\sum_{j=1}^{m} M_{ij}$$

Then the degree-of-freedom, degree of deviation for the observed urban growth over the expected (Table 8), was computed using the Pearson's expression: *(observed-expected)* ^{2}*/expected*.

The Pearson's chi-square statistics for each temporal interval (X_i^2) (Table 9) was then calculated using the observed (Table 5) and expected (Table 7) built-up growth as:

$$X_i^2 = \sum_{j=1}^{m} \frac{(M_j - M_j^E)^2}{M_j^E} \quad (2)$$

where X_i^2=degree-of-freedom for i^{th} temporal interval, M_j =observed built-up area in j^{th} column for a specific row, and M_j^E =expected built-up area in j^{th} column for a specific row.

Table 7. Expected growth of built-up area (ha)

	N	NE	E	SE	S	SW	W	NW
1987-1999	32.52	41.50	44.50	133.49	137.84	18.70	9.18	3.96
1999-2011	77.60	99.06	106.22	318.59	328.96	44.62	21.90	9.44

Similarly, substituting j (column) by i (row) and m (number of columns) by n (number of rows) in Equation (2) will yield the degree-of-freedom for each zone (X_j^2) (Table 10). The overall degree-of-freedom (X^2) was also estimated using Equation (3) and shown in Table 15.

$$X^2 = \sum_{i=1}^{n}\sum_{j=1}^{m} \frac{(M_{ij} - M_{ij}^E)^2}{M_{ij}^E} \quad (3)$$

From Equation (2), we found that chi-square has a lower limit of zero when the observed value is exactly the same as the expected value. It is evident that the degree-of-freedom for each temporal interval (Table 9) was found very high which explains the high variation between the observed and expected urban growth. Table 10 also revealed that the degree-of-freedom in the East and South zones was low portraying the similarity in

observed and expected urban growth. Higher overall degree-of-freedom indicates lack of consistent planned development in the city under investigation over time (Bhatta et al., 2010a; Bhatta, 2012), and it cannot be considered as sprawl, but as disparity in observed and expected growth in pattern and /or process.

Table 8. Difference between observed and expected built-up growth (ha)

	N	NE	E	SE	S	SW	W	NW
1987-1999	16.00	-7.86	5.74	-34.37	-9.40	12.86	10.46	6.56
1999-2011	-16.00	7.86	-5.74	34.37	9.40	-12.86	-10.46	-6.56

Table 9. Degree-of-freedom for urban growth in each temporal interval

Temporal interval	Freedom (X_i^2)
1987-1999	51.26
1999-2011	21.48

Table 10. Degree-of-freedom for urban growth in each zone

Zone	N	NE	E	SE	S	SW	W	NW
Freedom (X_j^2)	11.18	2.11	1.05	12.56	0.91	12.56	16.93	15.45

3.3 Shannon's Entropy and Urban Growth

Shannon's entropy is a widely applied method in studies of urban sprawl and it measures the degree of spatial concentration or dispersion of a geographical variable, observed built-up growth rates in zones (Yeh & Li, 2001; Li & Yeh, 2004; Sudhira et al., 2004; Almeida et al., 2005; Kumar, Pathan, & Bhanderi, 2007; Bhatta et al., 2010; Sarvestani et al., 2011). Shannon's entropy for each temporal interval (H_i) was calculated, from Table 6, as:

$$H_i = -\sum_{j=1}^{m} P_j log_e(P_j) \quad (4)$$

where (P_j) =proportion of the variable in the j^{th} column (i.e., proportion of built-up growth rate in j^{th} zone, calculated from Table 6) as: *(built-up growth rate in j^{th} zone/sum of built-up growth rates for all zones)*, m=total number of zones=8.

The entropy values range from 0 to $log_e(m)$ and its magnitude explains the degree of sprawl with values closer to 0 indicating a compact built-up growth distribution. Conversely, an evenly dispersed distribution among the zones will yield a value closer to $log_e(m)$.

When the entropy values are much higher than the half-way mark of $log_e(m)$, the city is said to be sprawled where as if such values goes below the half-way mark of $log_e(m)$, then it is non-sprawling (Bhatta et al., 2010a). It has to be noted that there was no reliable method found to define a threshold value that can determine whether a city is sprawled or not.

Table 11. Shannon's entropy of each temporal interval

Temporal interval	Entropy (H_i)	$\log_e(m)$	$\log_e(m)/2$
1987-1999	1.76	2.08	1.04
1999-2011	1.65	2.08	1.04

The result (Table 11) indicated that the entropy values are higher than the half-way mark of $log_e(m)$ asserting the city was sprawled. Comparing the entropy values of the temporal intervals, we found that there was a tendency of decrease in sprawl. This result corroborates the findings of Richardson, Bae, and Baxamusa (2000) and Bhatta et al. (2010a) that cities in developing countries are becoming more compact in spite of the beginnings of decentralization.

Similarly, entropy for each zone (H_j) given in Equation (5) was estimated by substituting i with j and m with n in Equation (4):

$$H_j = -\sum_{i=1}^{n} P_i log_e(P_i) \quad (5)$$

where P_i =proportion of the variable in the i^{th} row (i.e., proportion of built-up growth rate in i^{th} temporal interval, calculated from Table 6 as: *(built-up growth rate in i^{th} temporal interval/sum of built-up growth rates for all temporal intervals)*, n=total number of temporal intervals.

Table 12. Shannon's entropy for each zone

Zone	N	NE	E	SE	S	SW	W	NW
Entropy (H_j)	0.69	0.59	0.68	0.69	0.69	0.66	0.59	0.43
$log_e(n)$	0.69	0.69	0.69	0.69	0.69	0.69	0.69	0.69
$log_e(n)/2$	0.35	0.35	0.35	0.35	0.35	0.35	0.35	0.35

Table 12 indicated that the entropy values for each zone are all higher than the half-way mark of $log_e(n)$. This shows that the Hawassa City has a general tendency of sprawling. The lowest sprawl was observed in NW zone where the expansion of built-up area is limited by a natural barrier, the Lake. The sprawling effects in the N and NE for temporal instant in 2011 are mainly attributable to illegal settlements. These illegal settlements account for about 19.8% and 14.5% of built-up areas in the N and NE zones respectively.

The overall sprawl (H) can also be computed as given by Equation (6):

$$H = -\sum_{i=1}^{n}\sum_{j=1}^{m} P_{ij} log_e(P_{ij}) \quad (6)$$

where P_{ij} =proportion of the variable in the i^{th} row and j^{th} column (i.e., proportion of built-up growth rate in i^{th} temporal interval and j^{th} zone, calculated from Table 6 as: *(built-up growth rate in i^{th} temporal interval and j^{th} zone/the grand total of all variables)*.

The result of the overall sprawl calculated was 2.4 and found higher than the half-way mark of $log_e(nxm)$ i.e. 1.39. The upper limit of the overall sprawl is considered to be $log_e(nxm) = 2.77.$ which portrays that Hawassa City has an overall sprawled pattern.

3.4 Degree-of- Goodness and Urban Growth

Chi-square and entropy were used to measure degree-of-freedom and sprawl respectively. However, these are not enough to decide "goodness" of the urban growth. This is exemplified by the South zone where the observed and expected growth rates (X_j^2) are relatively related, but still the extent of sprawl (H_j) is one of the highest. Therefore, this requires determining the degree-of-goodness of the urban growth. The degree-of-goodness actually refers to the degree to which observed growth relates to the planned growth and the magnitude of compactness as opposed to sprawl (Bhatta, 2012).

The degree-of-goodness for each temporal interval (G_i) was calculated as:

$$G_i = log_e\left[\frac{1}{X_i^2\left(\frac{H_i}{log_e(m)}\right)}\right] \quad (7)$$

where (G_i) = degree-of-goodness, (X_i^2)=degree-of-freedom, and (H_i) = entropy all for the i^{th} temporal interval, and m =total number of zones=8. The result is given in Table 13.

Similarly, the degree-of-goodness for each zone (G_j) (Table 14) was computed by substituting i with j and m with n in Equation (7).

To compare the degree-of-goodness of the city, an overall degree-of-goodness was also estimated using Equation (8):

$$G = log_e\left[\frac{1}{X^2\left(\frac{H}{log_e(nxm)}\right)}\right] \quad (8)$$

where X^2 is an overall freedom and H is an overall sprawl (Table 15)

Table 13. Degree-of-goodness for urban growth in each temporal interval

Temporal interval	Goodness (G_i)
1987-1999	-3.77
1999-2011	-2.84

Table 14. Degree-of-goodness for urban growth in each zone

Zone	N	NE	E	SE	S	SW	W	NW
Goodness (G_j)	-2.41	-0.58	**-0.03**	-2.53	**0.10**	-2.48	-2.67	-2.25

The magnitude and algebraic signs of the degree-of-goodness are direct indications of whether the urban growths investigated in the temporal intervals or zones are "good" or "bad". Positive values indicate "goodness" while negative values indicate "badness" of the urban growth. Higher magnitude in degree-of-goodness also shows the badness of the urban growth. Based on the analysis (Table 13), the study area has not experienced goodness during the entire study period, the worst being during the 1987-1999. The analysis for the zones also indicated that, except for South, the values of degree-of-goodness of all zones were with negative sign. The worst is again the West zone, but the overall degree-of-goodness is even much worse. This finding is also in line with the findings of Bhatta et al. (2010a). However, the review of literature did not find any research output that explored urban growth status in this study area.

Table 15. Overall degree-of-freedom, entropy, and degree-of-goodness

Degree-of-freedom (X^2)	Entropy (H)	Degree-of-goodness (G)
72.74	2.40	-4.14

This study considered a circular area equidistant from the city center, assuming that the expansion of urban growth will be equal in every direction from the center. However, uneven growth was observed caused by terrain variables. This effect was particularly visible from the left side of N-S line where the expansion of built-up area was impeded mainly by Lake Hawassa.

The utilized models could be applied for less or more zonal divisions that include both built-up and non-built-up areas. Dividing the area into a higher number of zones will statistically yield more reliable results. But this may reduce the expected values of built-up areas, variables, to less than five which are not recommended in Chi-square statistics (Larson & Farber, 2009). We can also agree with the arguments of Bhatta et al. (2010a) which stipulate that it would be better if the three measures ($X^2, H, and\ G$) were calculated on the basis of percentage of built-up area within a zone by excluding non-developable land. However, quantifying non-developable land from remote sensing data will not be practical due to lack of basic information regarding non-developable land and this could be one limitation of the models used in this study.

Since these kinds of urban growth analyses were not available for the study area, it is presumed that the employed methods and the achieved results will be useful for local planning authorities to recognize and manage urban growth. The results will particularly be useful to understand the current growth status of the city and establish investment goals that will enable to work towards planned development and service provision in the future. When repetitive Landsat and SPOT images of the same scene overtime are available, it is also possible to apply the methods used in this paper for regional planning. Because the utilization of remote sensing techniques and analytical models permits us quantify urban growth, understand the rate and trends of growth which would help in regional planning for better supply of infrastructure and other communication networks.

4. Conclusion

Built-up area was extracted from temporal remote sensing data and used to analyze the status of urban growth and sprawl. Quantifying urban growth and sprawl was performed using Chi-square statistics, Shannon's entropy and a model to characterize the degree-of-goodness. Such relatively simplified analytical models can easily be applied by city managers and planners who are not necessarily scientists. The approaches followed by sub-dividing the area into different zones have produced a detailed report on urban growth status which will be useful to device

mitigation strategies not only for the whole area as an entity, but will also enable the development of different planning policies for each zone with diverse effects.

It was very remarkable, but not unexpected, to see the gap between the rate of urban growth and population growth. Census results revealed that from 1987 to 2011, the population of Hawassa City increased from 41 138 to 313 546 (662.2%) which is a rate close to three times the growth of built-up area (234.5%) for the same period. Recognizing that all the built-up areas were not occupied by residential buildings, one can imagine the high number of occupants per house and the low mean living space available per person. However, this is another topic which requires further investigation to address the problems.

The study area is experiencing more dispersed urban growth at the expense of agricultural land where vertical expansion was rarely practiced during previous years. The major conversion to built-up area is from agricultural land and one of the limitations to the vertical expansion is the location disadvantage that it is found in an active seismic zone.

In conclusion, regular monitoring of urban growth status using multi-resolution and multi-temporal remote sensing data is highly desirable. This coupled with proper planning and sound land law will be useful to prevent illegal settlement and undesirable urban expansion that hinders the provision of basic services.

Acknowledgements

This research was funded by Norwegian Agency for Development Cooperation as part of capacity building at the Hawassa University and we are grateful for the provided financial support. We also would like to extend our gratitude to the University of Life Sciences, Hawassa University and all those who have supported us during data collection.

References

Abebe, Y. D., & Geheb, K. (Eds.). (2003). *Wetlands of Ethiopia. Proceedings of a seminar on the resources and status of Ethiopia's Wetlands, vi, 116*. Nairobi, IUCN-EARO Publication service.

Almeida, C. M., Montero, A. M. V., Mara, G., Soares-Filho, B. S., Cerqueira, G. C. …. Batty, M. (2005). GIS and remote sensing as tools for the simulation of urban land-use change. *International Journal of Remote Sensing, 26*, 759–774. http://dx.doi.org/10.1080/0143116051233131685

Assefa, G., Alemu, T., & Abinet, A. (2011). Hawassa city administration finance & economic development data collection and dissemination work-process. *Socio-economic Profile - 2003EC, p-9*.

Aynalem, A. (2011). *Migration and urbanization*. Retrieved from http://www.EthiopianDemographyAndHealth.org

Barnes, K. B., Morgan, J. M., Roberge, M. C., & Lowe, S. (2002). *Sprawl development: Its patterns, consequences, and measurement. Towson University*. Retrieved from http://pages.towson.edu/morgan/files/Sprawl_Development.pdf

Bhatta, B., Saraswati, S., & Bandyopadhyay, D. (2010a). Quantifying the degree-of-freedom, degree-of-sprawl, and degree-of-goodness of urban growth from remote sensing data. *Applied Geography, 30*, 96-111. http://dx.doi.org/10.1016/j.apgeog.2009.08.001

Bhatta, B., Saraswati, S., & Bandyopadhyay, D. (2010b). Urban sprawl measurement from remote sensing data. *Applied Geography, 30*, 731–740. http://dx.doi.org/10.1016/j.apgeog.2010.02.002

Bhatta, B. (2012). *Urban growth analysis and remote sensing*. Springer briefs in Geography, Kolkata. http://dx.doi.org/10.1007/978-94-007-4698-5

BOFED. (2011). *Bureau of Finance & Economic Development*. Regional statistical abstract, Hawassa.

Congalton, R. G. (2001). Accuracy assessment and validation of remotely sensed and other spatial information. *International Journal of Wildland Fire, 10*, 321–328. http://dx.doi.org/10.1071/WF01031

Congalton, R. G., & Green, K. (2009). *Assessing the accuracy of remotely sensed data: Principles and practices* (2nd Ed.). Taylor & Francis Group, Boca Raton, FL.

CSA. (1988). *Central Statistical Agency*. Projected Population & Housing Census of Ethiopia, Addis Ababa.

CSA. (2011). *Central Statistical Agency*. Projected Population & Housing Census of Ethiopia, Addis Ababa.

ERDAS. (2010). *ERDAS Field Guide*. Erdas, Inc., Norcross, GA.

Galster, G., Hanson, R., Ratcliffe, M. R., Wolman, H., Coleman, S., & Freihage, J. (2001). Wrestling sprawl to the ground: Defining and measuring an elusive concept. *Housing Policy Debate, 12*, 681. http://dx.doi.org/10.1080/10511482.2001.9521426

Grey, W. M. F., Luckman, A. J., & Holland, D. (2003). Mapping urban change in the UK using satellite radar interferometry. *Remote Sensing of Environment, 87*, 16-22. http://dx.doi.org/10.1016/S0034-4257(03)00142-1

Hurni, H., Amare, B., Herweg, K., Portner, B., & Veit, H., (Eds.). (2007). Landscape transformation and sustainable development in Ethiopia. *Background information from a study tour through Ethiopia*, 4-20 September 2006, Compiled by the participants. Center for development and environment, University of Bern, Bern.

Jat, M. K., Garg, P. K., & Khare, D. (2008). Monitoring and modelling of urban sprawl using remote sensing and GIS techniques. *International Journal of Applied Earth Observation and Geoinformation, 10*, 26–43. http://dx.doi.org/10.1016/j.jag.2007.04.002

Ji, W., Ma, J., Twibell, R. W., & Underhill, K. (2006). Characterizing urban sprawl using multi-stage remote sensing images and landscape metrics. *Computers, Environment and Urban Systems, 30*, 861-879. http://dx.doi.org/10.1016/j.compenvurbsys.2005.09.002

Johnson, M. P. (2001). Environmental impacts of urban sprawl: a survey of the literature and proposed research agenda. *Environmental Planning, 33*, 717-73. http://dx.doi.org/10.1016/a3327

Karanja, F. N., Heipke, C., & Konecny, G. (2002). *Use of knowledge based systems for the detection & monitoring of unplanned developments* (Unpublished doctoral dissertation). University of Hannover, Hannover, Germany.

Kumar, J. A. V., Pathan, S. K., & Bhanderi, R. J. (2007). Spatio-temporal analysis for monitoring urban growth-a case study of Indore city. *Journal of the Indian Society of Remote Sensing, 35*(1).

Larson, R., & Farber, B. (2009). Elementary statistics, picturing the world (4th ed.). Pearson Prentice Hall, New Jersey, NJ.

Li, X., & Yeh, A. G. (2004). Analyzing spatial restructuring of land use patterns in a fast growing region using remote sensing and GIS. *Landscape and Urban Planning, 69*, 335–354. http://dx.doi.org/10.1016/j.landurbplan.2003.10.033

Lillesand, T. M., & Kiefer, R. W. (2000). *Remote sensing and image interpretation* (4th Ed.). John Wiley & Sons Inc., USA.

Mas, J. F. (1999). Monitoring land-cover changes: A comparison of change detection techniques. *Int. J. Remote Sensing, 20*, 139-152. http://dx.doi.org/10.1080/014311699213659

Mather, P. M. (1987). *Computer processing of remotely-sensed images: An introduction*. St. Edmundsbury Press Ltd., St. Edmunds, Suffolk.

Paul, S., & Dasgupta, A. (2013). Spatio-temporal analysis to quantify urban sprawl using geoinformatics. *International Journal of Advances in Remote Sensing and GIS, 1*, 3.

Richardson, H. W., Bae, C. C., & Baxamusa, M. H. (2000). Compact cities in developing countries: Assessment and implications. In M. Jenks & R. Burgess (Eds.), *Compact cities: Sustainable urban forms for developing countries*. Spon Press, London & New York.

Rozenstein, O., & Karineli, A. (2011). Comparison of methods for land-use classification incorporating remote sensing and GIS inputs. *Applied Geography, 31*, 533-544. http://dx.doi.org/10.1016/j.apgeog.2010.11.006

Sarvestani, M. S., Ibrahim, A. L., & Kanaroglou, P. (2011). Three decades of urban growth in the city of Shiraz, Iran: A remote sensing and geographic information systems application. *Cities, 28*, 320–329. http://dx.doi.org/10.1016/j.cities.2011.03.002

Sudhira, H. S., Ramachandra, T. V., & Jagadish, K. S. (2004). Urban sprawl: Metrics, dynamics and modelling using GIS. *International Journal of Applied Earth Observation and Geoinformation, 5*, 29–39. http://dx.doi.org/10.1016/j.jag.2003.08.002

Wondrade, N., Dick, Ø. B., & Tveite, H. (2014). GIS based mapping of land cover changes utilizing multi-temporal remotely sensed image data in Lake Hawassa Watershed, Ethiopia. *Environmental Monitoring and Assessment, 186*, 1765-1780. http://dx.doi.org/10.1007/s10661-013-3491-x

World Resources. (1996). *A guide to the global environment: The urban environment 1996-97*. Oxford University Press, Oxford.

Xiao, J., Shen, Y., Ge, J., Tateishi, R., Tang, C., Lilang, Y., & Huang, Z. (2006). Evaluating urban expansion and land use change in Shijiazhuang, China, using GIS and remote sensing. *Landscape and Urban Planning, 75*, 69-80. http://dx.doi.org/10.1016/j.landurbplan.2004.12.005

Yeh, A. G., & Li, X. (2001). Measurement and monitoring of urban Sprawl in a rapidly growing region using Entropy. *Photogrammetric Engineering & Remote Sensing, 67*, 83-90.

Zanganeh Shahraki, S., Sauri, D., Serra, P., Modugno, S., Seifolddini, F., & Pourahmad, A. (2011). Urban sprawl pattern and land-use change detection in Yazd. *Habitat International, 35*, 521-528. http://dx.doi.org/10.1016/j.habitatint.2011.02.004

Zeleke, K., & Serkalem, A. (2006). *History of Hawassa, 1960-2006*. Tony Printing Services, Hawassa.

ALLREFER. (1991). *Urbanization*. Retrieved February 27, 2013, from http://reference.allrefer.com/country-guide-study/ethiopia/ethiopia55.html

Notes

Note 1. Kebele is the smallest administrative unit in Ethiopia, in this case, having an area ranging from 20ha to 2760ha.

Note 2. The terms Hawassa, Hawassa City, and Hawassa City Administration have been used synonymously.

Note 3. The terms built-up, urban and developed area are used interchangeably.